Dynamical Slowing-Down in an Ultrafast Photoinduced Phase Transition

Alfred Zong,[1] Pavel E. Dolgirev,[2] Anshul Kogar,[1] Emre Ergeçen,[1] Mehmet B. Yilmaz,[1] Ya-Qing Bie,[1,*] Timm Rohwer,[1,†] I-Cheng Tung,[3] Joshua Straquadine,[4] Xirui Wang,[1] Yafang Yang,[1] Xiaozhe Shen,[5] Renkai Li,[5] Jie Yang,[5] Suji Park,[5,6] Matthias C. Hoffmann,[7] Benjamin K. Ofori-Okai,[5] Michael E. Kozina,[5] Haidan Wen,[3] Xijie Wang,[5] Ian R. Fisher,[4] Pablo Jarillo-Herrero,[1] and Nuh Gedik[1,‡]

[1]*Department of Physics, Massachusetts Institute of Technology, Cambridge, Massachusetts 02139, USA*
[2]*Skolkovo Institute of Science and Technology, Skolkovo Innovation Center, 3 Nobel Street, Moscow, 143026, Russia and Department of Physics, Harvard University, Cambridge, Massachusetts 02138, USA*
[3]*Advanced Photon Source, Argonne National Laboratory, Argonne, Illinois 60439, USA*
[4]*Geballe Laboratory for Advanced Materials, Stanford University, Stanford, California 94305, USA, Department of Applied Physics, Stanford University, Stanford, California 94305, USA, and SIMES, SLAC National Accelerator Laboratory, Menlo Park, California 94025, USA*
[5]*SLAC National Accelerator Laboratory, Menlo Park, California 94025, USA*
[6]*Department of Materials Science and Engineering, Stanford University, Stanford, California 94305, USA*
[7]*Linac Coherent Light Source, SLAC National Accelerator Laboratory, Menlo Park, California 94025, USA*

(Received 22 January 2019; published 29 August 2019)

Complex systems, which consist of a large number of interacting constituents, often exhibit universal behavior near a phase transition. A slowdown of certain dynamical observables is one such recurring feature found in a vast array of contexts. This phenomenon, known as critical slowing-down, is well studied mostly in thermodynamic phase transitions. However, it is less understood in highly nonequilibrium settings, where the time it takes to traverse the phase boundary becomes comparable to the timescale of dynamical fluctuations. Using transient optical spectroscopy and femtosecond electron diffraction, we studied a photoinduced transition of a model charge-density-wave (CDW) compound $LaTe_3$. We observed that it takes the longest time to suppress the order parameter at the threshold photoexcitation density, where the CDW transiently vanishes. This finding can be captured by generalizing the time-dependent Landau theory to a system far from equilibrium. The experimental observation and theoretical understanding of dynamical slowing-down may offer insight into other general principles behind nonequilibrium phase transitions in many-body systems.

DOI: 10.1103/PhysRevLett.123.097601

In a second-order symmetry-breaking phase transition, the spatial extent of fluctuating regions diverges close to the critical temperature T_c. Correspondingly, the relaxation time of these fluctuations tends to infinity, a phenomenon known as critical slowing-down [1,2]. The phenomenology of slowing dynamics near a critical point is much more general: it has been observed in first-order transitions [3,4], glasses [5,6], dynamical systems [7], and even microbial communities [8]. Its common occurrence makes it a robust signature of phase transitions in a vast array of complex systems [9].

Close to equilibrium, critical slowing-down has been well characterized in condensed matter systems. Theoretically, it is described by a dynamical critical exponent, whose value depends on the dynamic universality class [2]. Experimentally, the evidence comes from a vanishing rate of change in the order parameter close to T_c, with early reports in Refs. [3,10,11]. While these measurements probe the slowing dynamics in the time domain, it can be observed in the frequency domain as well. For example, inelastic neutron scattering has revealed a narrowing quasielastic peak along the energy axis as T_c is approached, indicating a suppressed relaxation rate of critical fluctuations [12–14]. Moreover, if there is a collective mode associated with the phase transition, the mode softening in the vicinity of T_c is also taken as a signature of critical slowing-down [15].

For symmetry-breaking phase transitions in a highly nonequilibrium setting, the dynamics are much less understood. Recent studies have found important features in nonequilibrium transitions, such as topological defects, which are absent in their equilibrium counterparts [16–18]. Despite the differences, a slowdown in dynamics is thought to carry over to systems far from equilibrium. For example, in a rapid quench into a broken-symmetry state, the Kibble-Zurek theory suggests that critical slowing-down plays a central role in domain formation: as the phase boundary is traversed at a faster rate than the system can respond, spatially disconnected regions may adopt distinct configurations of the same degenerate ground state [19]. Characteristic domain structures in liquid crystals have

indeed been observed [20,21], providing indirect evidence for the slowdown.

To study the dynamics in a nonequilibrium setting, charge-density-wave (CDW) transitions instigated by an intense femtosecond laser pulse provide an accessible platform with well-controlled tuning parameters. A suite of time-resolved probes can track the evolution of electronic and lattice orders after strong photoexcitation [18], offering insights into the critical behavior, if present, during the phase transition. Immediately after photoexcitation, a coherently excited CDW amplitude mode was observed to soften transiently [16], hinting at critical slowing-down. Right below T_c, a diverging relaxation time back to equilibrium was interpreted as another signature [4,22]. However, observables in previous studies, such as amplitude mode frequency or quasiparticle relaxation time across the spectroscopic gap, are only well defined in the broken-symmetry state [23–25]. To demonstrate slowing dynamics in the vicinity of a nonequilibrium phase transition, ideally one would measure an increased timescale near the phase boundary compared to both ordered and disordered states.

In this work, we circumvent this obstacle by focusing on a different observable during the photoinduced melting of a CDW: the time taken to suppress the condensate. With increasing photoexcitation densities, the perturbed system will enter one of the two transient states, where the CDW is either partially or completely suppressed [18]. The two states are separated by the threshold excitation density F_{melt}, where the condensate first vanishes completely. Through transient reflectivity and time-resolved diffraction measurements at different excitation densities, we observed that it takes the maximum time to suppress the CDW right at F_{melt}, indicating dynamical slowing-down near the boundary between the two transient states. Here, we use *dynamical* slowing-down to emphasize the highly nonequilibrium nature of the system and to distinguish it from *critical* slowing-down commonly defined in a second-order phase transition in equilibrium [1,2].

The material of interest is a paradigmatic CDW system, $LaTe_3$ [26]. Like other rare-earth tritellurides, $LaTe_3$ possesses a quasi-2D structure [Fig. 1(a)] and develops a unidirectional CDW with wave vector $\mathbf{q}_{\mathrm{CDW}}$ along the c axis below $T_c \approx 670$ K [27]. In equilibrium, the CDW transition is characterized by the appearance of satellite peaks in a diffraction pattern (Fig. S1(b) in the Supplemental Material [28]) as well as gap openings at certain parts of the Fermi surface connected by $\mathbf{q}_{\mathrm{CDW}}$ [36].

Upon the arrival of a strong femtosecond laser pulse, the CDW order is transiently suppressed [18,37,38]. We first establish the timescale for this process by performing ultrafast electron diffraction (UED) and transient optical spectroscopy (TOS), which reveal how the lattice and electrons respond to intense photoexcitation, respectively [Fig. 1(a)]. Previous measurements from time- and angle-resolved photoemission spectroscopy (trARPES) [18] and time-resolved x-ray diffraction (trXRD) [37] are also included to obtain a comprehensive and consistent view of the ultrafast melting process.

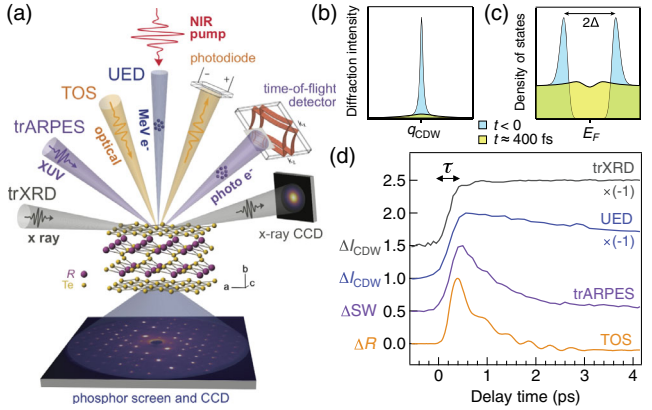

FIG. 1. Photoinduced CDW melting probed by multiple time-resolved techniques. (a) Schematics of time-resolved probes, including ultrafast electron diffraction (UED), transient optical spectroscopy (TOS), time- and angle-resolved photoemission spectroscopy (trARPES), and time-resolved x-ray diffraction (trXRD). The full electron diffraction pattern is shown in Fig. S1(b) in the Supplemental Material [28]. (b),(c) Schematics of the superlattice peak and density of states before (blue) and after (yellow) photoexcitation. (d) Transient response of superlattice peak intensity (ΔI_{CDW}), in-gap spectral weight (ΔSW), and reflectivity (ΔR) probed by corresponding time-resolved techniques. All traces are normalized between 0 and 1 and vertically offset for clarity. ΔI_{CDW} is inverted for easier comparison. All traces are measured in $LaTe_3$ except for trXRD, which measures $TbTe_3$, a similar compound in the same rare-earth tritelluride family with a lower T_c. The trace of trARPES is adapted from Ref. [18]. The trace of trXRD is adapted with permission from Ref. [37], copyrighted by the American Physical Society.

While UED and trXRD track the evolution of CDW satellite peaks at characteristic wave vector $\mathbf{q}_{\mathrm{CDW}}$ [Fig. 1(b)], TOS and trARPES probe the change in the spectroscopic gap [Fig. 1(c)] [18]. Despite the different observables, the initial response that corresponds to CDW melting proceeds with a similar timescale, denoted by τ [Fig. 1(d)]. The rising edges across the four techniques in Fig. 1(d) all span a time interval of $\tau \approx 400$ fs, with variations arising from the different temporal resolutions in each setup [28] and different photoexcitation densities used [Fig. 2(d)]. The agreement among structural and electronic probes suggests the presence of strong electron-phonon coupling in this system. Notably, the value of 400 fs is on the same scale as the period of the 2.2 THz CDW amplitude mode [25], further indicating the vital role of lattice vibrations in the formation of the charge order [39].

Among the four techniques discussed, TOS possesses the best temporal resolution and signal-to-noise ratio [28]. Hence, it enables us to more quantitatively investigate the

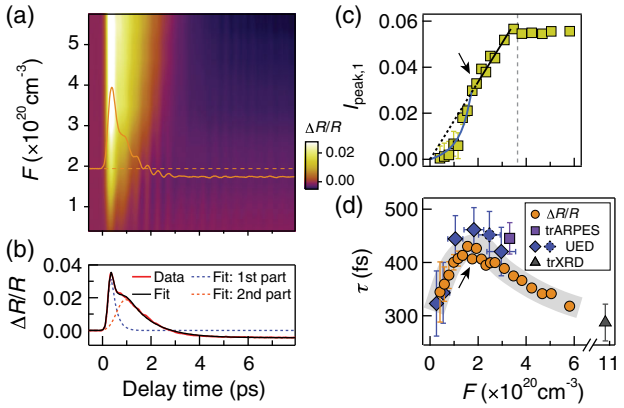

FIG. 2. CDW suppression time at different excitation densities. (a) $\Delta R/R$ traces at different excitation densities F expressed in terms of absorbed photons per unit volume. A particular $\Delta R/R$ cut is overlaid at the excitation density indicated by the dashed line. It is the same trace shown in Fig. 1(d). (b) $\Delta R/R$ trace at $F = 5.81 \times 10^{20}$ cm^{-3}, together with an example fit from Eq. (S1) in the Supplemental Material [28]. (c) Initial excited quasiparticle population $I_{\mathrm{peak},1}$ showing a superlinear dependence on F below F_{melt} (arrow) and a plateau beyond F_{bleach} (vertical dashed line). Black line is a linear fit with extrapolation (dashed) to zero. Blue curve is a fit to Eq. (S2) in the Supplemental Material [28]. (d) CDW suppression time τ as a function of excitation density F. Gray curve is a guide to eye. For the UED data, the corresponding trace of the dashed diamond is shown in Fig. 1(d) while the rest, measured on a separate sample, are shown in Fig. S2 in the Supplemental Material [28]. Error bars indicate uncertainties in curve fittings and in the instrumental temporal resolution [28].

timescale of CDW suppression τ as we vary the laser excitation density F quoted in terms of absorbed photon number per unit volume [18]. Figure 2(a) shows the temporal evolution of the transient reflectivity $\Delta R/R$ across a large range of F. The trace from Fig. 1(d) is overlaid at the corresponding F. The data presented were taken using a probe photon energy of 1.80 eV (690 nm), which is selected among the white light supercontinuum because it is the energy most sensitive to the dynamics of the CDW gap [28]. In Fig. 2(b), we present an example cut (red curve) at $F = 5.81 \times 10^{20}$ cm^{-3}. To quantitatively evaluate the initial response time τ, we performed a global fit for traces at all excitation densities using a two-component phenomenological model with minimal parameters. An example fit is presented in Fig. 2(b), showing excellent agreement. We attribute the two components to quasiparticle excitations in different parts of the Brillouin zone (see Ref. [28] for details of the fitting model and its interpretation), and we extract τ from the rise time of the first component [Fig. 2(b), blue dashed curve].

Remarkably, the rise time τ displays a nonmonotonic trend as a function of excitation density [Fig. 2(d), orange circles], with a maximum at $\sim 2 \times 10^{20}$ cm^{-3} (black arrow). The nonmonotonic trend of τ is independent of the fitting model, and is clearly observed in the raw data (Fig. S3(a) in the Supplemental Material [28]). To confirm this observation, we similarly track the suppression of superlattice peaks using UED at various excitation densities (Fig. 2(d), blue diamonds, and Fig. S2 in the Supplemental Material [28]). Despite significantly larger errors due to lower signal-to-noise ratio and poorer temporal resolution compared to the TOS measurements, the initial timescale in the UED experiments suggests the same nonmonotonic behavior in τ. We further note a recent measurement on $SmTe_3$ [40], a CDW compound in the same family as $LaTe_3$, which demonstrates a similar trend in the initial system response.

To associate this nonmonotonic behavior in τ with dynamical slowing-down during photoinduced CDW melting, we next establish that the melting proceeds the slowest precisely at the threshold excitation density when the CDW in the illuminated sample volume is just fully destroyed; namely, $F_{\mathrm{melt}} \approx 2 \times 10^{20}$ cm^{-3}. We make three observations in this regard. First, the value 2×10^{20} cm^{-3} corresponds to the point where the superlattice peak is observed to completely disappear in UED measurements [18], suggesting that τ indeed peaks at the threshold excitation density. Second, the time for the initial fast relaxation in transient reflectivity displays a steeply increasing trend at F_{melt} (Fig. S3(c) in the Supplemental Material [28]). This is attributed to a vanishing energy gap at the Fermi level when the CDW is completely suppressed, which limits the decay rate of excited quasiparticles [23–25]. Third, the maximum reflectivity change $I_{\mathrm{peak},1}$ also displays distinct behavior below and above F_{melt} [Fig. 2(c)]. Below F_{melt}, the presence of a CDW gap modifies the transient population of excited quasiparticles, resulting in a superlinear $I_{\mathrm{peak},1}$ as a function of excitation density [Fig. 2(c), blue curve; see Ref. [28]]. Beyond F_{melt}, the excited quasiparticle population is directly proportional to the excitation density [Fig. 2(c), black line]. Above an even higher value F_{bleach}, the peak reflectivity $I_{\mathrm{peak},1}$ plateaus [Fig. 2(c), vertical dashed line] due to quasiparticle bleaching [28]. It is worth emphasizing that at F_{melt}, the lattice temperature stays below T_c at all time delays after photoexcitation [18], reaffirming that the observed CDW melting is nonthermal in nature and not a result of transient lattice heating above the transition temperature.

To interpret the nonmonotonic trend of the initial response time (τ) measured in TOS, we need to understand what physical quantity is probed by transient reflectivity. Unlike the superlattice peak intensity in diffraction measurements or in-gap spectral weight in trARPES, optical reflectivity is not a direct gauge of the CDW order parameter. Typically, in a gapped system, the value of transient reflectivity is taken to be proportional to the excited quasiparticle density [23–25], which in turn is sensitive to the gap size. For example, clear oscillations are present in ΔR traces (Figs. 1(d), 2(a), and Fig. S4 in the

Supplemental Material [28]), with a dominant contribution from the CDW amplitude mode [25]—the modulation of the gap magnitude. Based on this sensitivity of ΔR to the gap size as well as the consistency of the initial timescale in Figs. 1(d) and 2(d) across techniques, we take the initial rise time (τ) in transient reflectivity as the time needed for the amplitude of the CDW order parameter to be maximally suppressed. The value of τ is well separated from any electron-electron scattering timescale ($\lesssim$100 fs) [23,41], and represents a simultaneous population of excited quasiparticles and renormalization of the gap, which occur self-consistently.

Having established the precise meaning of τ, we draw some parallels between the present nonequilibrium study and its equilibrium counterparts to interpret the observation in Fig. 2(d). At equilibrium, when the temperature is close to T_c, time-domain measurements of the order parameter indicate a reduced rate of change, which signifies critical slowing-down [3,10,11]. Here, we use photoexcitation density in lieu of temperature as the tuning parameter, and we extend the timescale to the femtosecond regime. Similarly, we interpret the maximum value of τ at exactly the threshold excitation density as a signature of dynamical slowing-down in this ultrafast phase transition.

To understand how a slowdown in dynamics can be extended to a regime far from equilibrium, we again make reference to the established framework of symmetry-breaking transition in equilibrium, which is parametrized by an order parameter ψ. On a phenomenological level, we consider the standard Landau potential, $\mathcal{W}(\psi) = -\alpha|\psi|^2 + (\beta/2)|\psi|^4$, which gives the simplest description of the second-order CDW transition in $LaTe_3$ [26]; here, α, β are the usual Landau coefficients. To see the slowdown near T_c, the typical treatment is to solve the time-dependent Landau equation [2], $\partial\psi/\partial t = -\Gamma\delta\mathcal{W}/\delta\psi + \eta(t)$, where Γ is a phenomenological parameter and $\eta(t)$ is the Langevin noise term representing fluctuations. Close to T_c, where the order parameter ψ is small and the free energy $\mathcal{W}(\psi)$ develops a flat bottom, the relaxation time of long-wavelength fluctuations in ψ can be shown to approach infinity, which is the origin of critical slowing-down [2].

We now generalize this treatment to a highly nonequilibrium regime. To account for the different responses by the electronic and phononic subsystems, we consider two components, one for the electrons (ψ_e) and the other for the lattice (ψ_l). The Landau free-energy functional is [2,28,42–44]

$$\mathcal{W} = -\alpha_e|\psi_e|^2 + \frac{\beta}{2}|\psi_e|^4 - \zeta(\psi_e\psi_l^* + \psi_e^*\psi_l) + \alpha_l|\psi_l|^2. \tag{1}$$

Here, α_e, α_l, and β are model parameters; the $\zeta(\cdot)$ term represents electron-phonon coupling. The equations of motion are given by

$$\frac{d\psi_e}{dt} \propto -\frac{\delta\mathcal{W}}{\delta\psi_e} \quad \text{and} \quad \frac{d^2\psi_l}{dt^2} \propto -\frac{\delta\mathcal{W}}{\delta\psi_l}, \tag{2}$$

where the electronic dynamics is similar to that in the equilibrium treatment and heavy lattice ions are assumed to behave like classical oscillators. Detailed discussion of the model and the numerical solution to Eq. (2) are described in Ref. [28]; here, we only highlight the physical picture summarized in Fig. 3(a). Unlike the equilibrium case where microscopic fluctuations, captured by $\eta(t)$, initiate the dynamics, the temporal evolution in the nonequilibrium case is driven by a femtosecond laser pulse, where a coherently excited CDW amplitude mode plays an instrumental role [39]. The pulse modifies the free-energy functional [α_e in Eq. (1)] and sets off the order parameter to seek a new global minimum. Though we draw the free energy as fixed curves, it should be noted that it evolves dynamically according to Eq. (S6) in the Supplemental Material [28]. As the dynamics of ψ_e and ψ_l closely follow each other [28], we use a single circle to denote the order parameter in Fig. 3(a). At the critical excitation density F_{melt}, beyond which the order parameter vanishes transiently, the time taken to suppress the order is the longest [$\tau_2 > \tau_1, \tau_3$ in Fig. 3(a)]. Similar to the equilibrium situation, the slow evolution reflects a transiently flat potential landscape when the order parameter is close to zero, which leads to its reduced rate of change.

Using our experimental parameters for the time-dependent Landau equation, the calculated CDW suppression time τ is shown in Fig. 3(b). There is no adjustable parameter except a constant that converts a dimensionful F in the experiment to a dimensionless quantity in the computation. Here, τ is defined as the time spanned

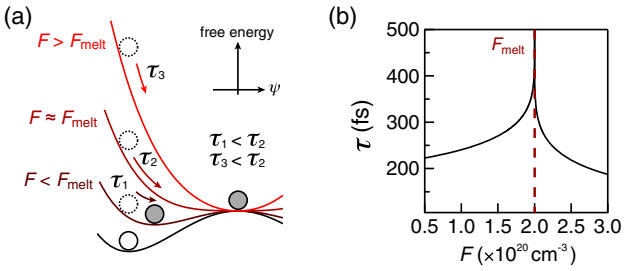

FIG. 3. Dynamical slowing-down in the generalized time-dependent Landau theory. (a) Schematic of CDW order parameter (ψ) dynamics in a Landau free-energy landscape. The solid circle represents ψ before photoexcitation and dashed circles are nonequilibrium ψ in an impulsively altered free energy, whose subsequent evolution, which is not drawn, is described by Eq. (S6) in the Supplemental Material [28]. Filled circles represent ψ when CDW is transiently suppressed, either partially or completely. Colored curves are snapshots of transient free energies at different excitation densities right after laser pulse incidence. At F_{melt}, ψ first reaches zero in its temporal evolution. (b) Calculated CDW suppression time as a function of excitation density, based on the time-dependent Landau formalism [28].

between the arrival of the laser pulse and the transient minimum position of order parameter amplitude. It shows a distinct peak at the critical point F_{melt}, which captures the experimental observation in Fig. 2(d). Notably, the absolute value of the calculated τ falls under a similar range of magnitudes as observed in the experiment. This timescale is determined by the period of the CDW amplitude mode in the simulation [28], indicating the instrumental role of phonons in mediating the ultrafast transition.

There is one key difference between the calculated and measured trend of τ: the latter lacks a sharp divergence at the threshold excitation density. We attribute this rounding of the divergence to the presence of temporally or spatially varying perturbations on the system, such as photoinduced topological defects [16–18] or additional phonons coupled to the CDW order [25,37,45], which are not considered in our minimal model. In the Landau picture, they disrupt the flat potential energy landscape when the order parameter approaches zero, which is required for the diverging behavior. Furthermore, the divergence only happens in a very narrow window of excitation densities [Fig. 3(b)], which makes experimental detection challenging, as any small uncertainties or fluctuations in the pulse energy can smear the singularity.

In conclusion, two different time-resolved probes are used to systematically study the ultrafast melting of a CDW instigated by an intense laser pulse. We have experimentally demonstrated the phenomenon of dynamical slowing-down, manifested as the longest time it takes to suppress the CDW at the threshold excitation density in the non-equilibrium phase transition. The agreement in timescale across techniques and with theoretical simulation by time-dependent Landau equations highlights the important role of phonons in this photoinduced transition. Despite complexities involved in phase transitions far from equilibrium, the observation of slowing dynamics in this setting pinpoints a robust commonality for us to understand non-equilibrium phenomena of more intricate systems.

We acknowledge helpful discussions with B. V. Fine, A. V. Rozhkov, and E. Baldini. We thank E. J. Sie for assistance in sample handling. We acknowledge support from the U.S. Department of Energy, BES DMSE (experimental setup and data acquisition), from the Gordon and Betty Moore Foundation's EPiQS Initiative Grant No. GBMF4540 (data analysis and manuscript writing), and the Skoltech NGP Program (Skoltech-MIT joint project) (theory). I-C. T. and H. W. acknowledge support from the U.S. Department of Energy, Office of Science, Office of Basic Energy Sciences, under Contract No. DE-SC0012509 (data acquisition). Y.-Q. B. was supported by the Center for Excitonics, an Energy Frontier Research Center funded by the U.S. Department of Energy, Office of Science, Office of Basic Energy Sciences, under Award No. DESC0001088 (sample characterization). Y. Y. was supported by the Center for Integrated Quantum Materials under NSF Grant No. DMR-1231319 (device fabrication). Research in the P. J.-H. group (Y.-Q. B., Y. Y., Xirui Wang., and P. J.-H.) was partially supported by the Gordon and Betty Moore Foundation's EPiQS Initiative through Grant No. GBMF4541 (sample preparation and characterization). J. S. and I. R. F. acknowledge support from the U.S. Department of Energy, Office of Basic Energy Sciences, under Contract No. DE-AC02-76SF00515 (sample growth and characterization). X. S., R. L., J. Y., S. P., M. C. H., B. K. O.-O., M. E. K., and Xijie Wang. acknowledge support by the U.S. Department of Energy BES SUF Division Accelerator and Detector R&D program, the LCLS Facility, and SLAC under Contracts No. DE-AC02-05-CH11231 and No. DE-AC02-76SF00515 (MeV UED).

*Present address: School of Electronics and Information Technology, Sun Yat-sen University, Guangzhou, Guangdong 510006, China.

†Present address: Center for Free-Electron Laser Science, DESY, Notkestraße 85, 22607 Hamburg, Germany.

‡Corresponding author.
gedik@mit.edu

[1] M. F. Collins, *Magnetic Critical Scattering* (Oxford University Press, Oxford, 1989).

[2] N. Goldenfeld, *Lectures on Phase Transitions and the Renormalization Group* (Addison-Wesley, Boston, 1992).

[3] Y. Horie, T. Fukami, and S. Mase, First order structural phase transition in $BaPb_{1-x}Bi_xO_3$ and the scaling law, Solid State Commun. **62**, 471 (1987).

[4] Y. Zhu, J. Hoffman, C. E. Rowland, H. Park, D. A. Walko, J. W. Freeland, P. J. Ryan, R. D. Schaller, A. Bhattacharya, and H. Wen, Unconventional slowing down of electronic recovery in photoexcited charge-ordered $La_{1/3}Sr_{2/3}FeO_3$, Nat. Commun. **9**, 1799 (2018).

[5] J. Souletie and J. L. Tholence, Critical slowing down in spin glasses and other glasses: Fulcher versus power law, Phys. Rev. B **32**, 516 (1985).

[6] J. C. Lasjaunias, K. Biljaković, F. Nad', P. Monceau, and K. Bechgaard, Glass Transition in the Spin-Density Wave Phase of $(TMTSF)_2PF_6$, Phys. Rev. Lett. **72**, 1283 (1994).

[7] S. Strogatz, *Nonlinear Dynamics and Chaos: With Applications to Physics, Biology, Chemistry, and Engineering* (CRC Press, Boca Raton, 2018).

[8] A. J. Veraart, E. J. Faassen, V. Dakos, E. H. van Nes, M. Lürling, and M. Scheffer, Recovery rates reflect distance to a tipping point in a living system, Nature (London) **481**, 357 (2012).

[9] M. Scheffer, J. Bascompte, W. A. Brock, V. Brovkin, S. R. Carpenter, V. Dakos, H. Held, E. H. van Nes, M. Rietkerk, and G. Sugihara, Early-warning signals for critical transitions, Nature (London) **461**, 53 (2009).

[10] M. R. Collins and H. C. Teh, Neutron-Scattering Observations of Critical Slowing Down of an Ising System, Phys. Rev. Lett. **30**, 781 (1973).

[11] M. Iizumi, Real-time neutron diffraction studies of phase transition kinetics, Physica (Amsterdam) **136(B+C)**, 36 (1986).

[12] H. Cailleau, A. Heidemann, and C. M. E. Zeyen, Observation of critical slowing down at the structural phase transition in p-terphenyl by high-resolution neutron spectroscopy, J. Phys. C **12**, L411 (1979).
[13] B. Toudic, H. Cailleau, R. E. Lechner, and W. Petry, Direct Observation of Critical Phenomena by Incoherent Neutron Scattering, Phys. Rev. Lett. **56**, 347 (1986).
[14] W. Press, A. Hüller, H. Stiller, W. Stirling, and R. Currat, Critical Slowing Down of Orientational Fluctuations in a Plastic Crystal, Phys. Rev. Lett. **32**, 1354 (1974).
[15] D. Niermann, C. P. Grams, P. Becker, L. Bohatý, H. Schenck, and J. Hemberger, Critical Slowing Down Near the Multiferroic Phase Transition in $MnWO_4$, Phys. Rev. Lett. **114**, 037204 (2015).
[16] R. Yusupov, T. Mertelj, V. V. Kabanov, S. Brazovskii, P. Kusar, J.-H. Chu, I. R. Fisher, and D. Mihailovic, Coherent dynamics of macroscopic electronic order through a symmetry breaking transition, Nat. Phys. **6**, 681 (2010).
[17] T. Mertelj, P. Kusar, V. V. Kabanov, P. Giraldo-Gallo, I. R. Fisher, and D. Mihailovic, Incoherent Topological Defect Recombination Dynamics in $TbTe_3$, Phys. Rev. Lett. **110**, 156401 (2013).
[18] A. Zong, A. Kogar, Y.-Q. Bie, T. Rohwer, C. Lee, E. Baldini, E. Ergeçen, M. B. Yilmaz, B. Freelon *et al.*, Evidence for topological defects in a photoinduced phase transition, Nat. Phys. **15**, 27 (2019).
[19] W. Zurek, Cosmological experiments in condensed matter systems, Phys. Rep. **276**, 177 (1996).
[20] I. Chuang, R. Durrer, N. Turok, and B. Yurke, Cosmology in the laboratory: defect dynamics in liquid crystals, Science **251**, 1336 (1991).
[21] M. Bowick, L. Chandar, E. Schiff, and A. Srivastava, The cosmological Kibble mechanism in the laboratory: string formation in liquid crystals, Science **263**, 943 (1994).
[22] A. Tomeljak, H. Schäfer, D. Städter, M. Beyer, K. Biljakovic, and J. Demsar, Dynamics of Photoinduced Charge-Density-Wave to Metal Phase Transition in $K_{0.3}MoO_3$, Phys. Rev. Lett. **102**, 066404 (2009).
[23] J. Demsar, K. Biljaković, and D. Mihailovic, Single Particle and Collective Excitations in the One-Dimensional Charge Density Wave Solid $K_{0.3}MoO_3$ Probed in Real Time by Femtosecond Spectroscopy, Phys. Rev. Lett. **83**, 800 (1999).
[24] V. V. Kabanov, J. Demsar, B. Podobnik, and D. Mihailovic, Quasiparticle relaxation dynamics in superconductors with different gap structures: theory and experiments on $YBa_2Cu_3O_{7-\delta}$, Phys. Rev. B **59**, 1497 (1999).
[25] R. V. Yusupov, T. Mertelj, J.-H. Chu, I. R. Fisher, and D. Mihailovic, Single-Particle and Collective Mode Couplings Associated with 1- and 2-Directional Electronic Ordering in Metallic $R\,\mathrm{Te}_3 (R = \mathrm{Ho, Dy, Tb})$, Phys. Rev. Lett. **101**, 246402 (2008).
[26] N. Ru, C. L. Condron, G. Y. Margulis, K. Y. Shin, J. Laverock, S. B. Dugdale, M. F. Toney, and I. R. Fisher, Effect of chemical pressure on the charge density wave transition in rare-earth tritellurides $R\mathrm{Te}_3$, Phys. Rev. B **77**, 035114 (2008).
[27] B. F. Hu, B. Cheng, R. H. Yuan, T. Dong, and N. L. Wang, Coexistence and competition of multiple charge-density-wave orders in rare-earth tritellurides, Phys. Rev. B **90**, 085105 (2014).
[28] See Supplemental Material at http://link.aps.org/supplemental/10.1103/PhysRevLett.123.097601 for more experimental details and data analysis, which includes Refs. [29–35]. Section I, Details of time-resolved techniques; Sec. II, Determining UED temporal resolution by terahertz streaking; Sec. III, Fitting and interpretation of time traces; Sec. IV, Quasiparticle population across the gap below the critical excitation density; Sec. V, Probe photon energy in transient optical spectroscopy; Sec. VI, Time-dependent Landau theory.
[29] S. P. Weathersby, G. Brown, M. Centurion, T. F. Chase, R. Coffee, J. Corbett, J. P. Eichner, J. C. Frisch, A. R. Fry *et al.*, Mega-electron-volt ultrafast electron diffraction at SLAC National Accelerator Laboratory, Rev. Sci. Instrum. **86**, 073702 (2015).
[30] X. Shen, R. K. Li, U. Lundström, T. J. Lane, A. H. Reid, S. P. Weathersby, and X. J. Wang, Femtosecond mega-electron-volt electron microdiffraction, Ultramicroscopy **184**, 172 (2018).
[31] A. Sacchetti, L. Degiorgi, T. Giamarchi, N. Ru, and I. R. Fisher, Chemical pressure and hidden one-dimensional behavior in rare-earth tri-telluride charge-density wave compounds, Phys. Rev. B **74**, 125115 (2006).
[32] F. Pfuner, L. Degiorgi, J.-H. Chu, N. Ru, K. Y. Shin, and I. R. Fisher, Optical properties of the charge-density-wave rare-earth tri-telluride compounds: a view on $PrTe_3$, Phys. B **404**, 533 (2009).
[33] R. K. Li, M. C. Hoffmann, E. A. Nanni, S. H. Glenzer, M. E. Kozina, A. M. Lindenberg, B. K. Ofori-Okai, A. H. Reid, X. Shen, S. P. Weathersby *et al.*, Terahertz-based subfemtosecond metrology of relativistic electron beams, Phys. Rev. Accel. Beams **22**, 012803 (2019).
[34] B. K. Ofori-Okai, M. C. Hoffmann, A. H. Reid, S. Edstrom, R. K. Jobe, R. K. Li, E. M. Mannebach, S. J. Park, W. Polzin *et al.*, A terahertz pump mega-electron-volt ultrafast electron diffraction probe apparatus at the SLAC Accelerator Structure Test Area facility, J. Instrum. **13**, P06014 (2018).
[35] H.-M. Eiter, M. Lavagnini, R. Hackl, E. A. Nowadnick, A. F. Kemper, T. P. Devereaux, J.-H. Chu, J. G. Analytis, I. R. Fisher, and L. Degiorgi, Alternative route to charge density wave formation in multiband systems, Proc. Natl. Acad. Sci. U.S.A. **110**, 64 (2013).
[36] V. Brouet, W. L. Yang, X. J. Zhou, Z. Hussain, R. G. Moore, R. He, D. H. Lu, Z. X. Shen, J. Laverock, S. B. Dugdale *et al.*, Angle-resolved photoemission study of the evolution of band structure and charge density wave properties in $R\mathrm{Te}_3 (R = \mathrm{Y, La, Ce, Sm, Gd, Tb, and Dy})$, Phys. Rev. B **77**, 235104 (2008).
[37] R. G. Moore, W. S. Lee, P. S. Kirchman, Y. D. Chuang, A. F. Kemper, M. Trigo, L. Patthey, D. H. Lu, O. Krupin, M. Yi *et al.*, Ultrafast resonant soft x-ray diffraction dynamics of the charge density wave in $TbTe_3$, Phys. Rev. B **93**, 024304 (2016).
[38] F. Schmitt, P. S. Kirchmann, U. Bovensiepen, R. G. Moore, L. Rettig, M. Krenz, J.-H. Chu, N. Ru, L. Perfetti *et al.*, Transient electronic structure and melting of a charge density wave in $TbTe_3$, Science **321**, 1649 (2008).
[39] S. Hellmann, T. Rohwer, M. Kalläne, K. Hanff, C. Sohrt, A. Stange, A. Carr, M. M. Murnane, H. C. Kapteyn *et al.*,

Time-domain classification of charge-density-wave insulators, Nat. Commun. **3**, 1069 (2012).

[40] M. Trigo, P. Giraldo-Gallo, M. E. Kozina, T. Henighan, M. P. Jiang, H. Liu, J. N. Clark, M. Chollet, J. M. Glownia, D. Zhu *et al.*, Coherent order parameter dynamics in $SmTe_3$, Phys. Rev. B **99**, 104111 (2019).

[41] J. Demsar and T. Dekorsy, Carrier dynamics in bulk semiconductors and metals after ultrashort pulse excitation, in *Optical Techniques for Solid-State Materials Characterization*, edited by R. Prasankumar and A. Taylor (CRC Press, Boca Raton, 2016), pp. 291–328.

[42] H. Schäfer, V. V. Kabanov, M. Beyer, K. Biljakovic, and J. Demsar, Disentanglement of the Electronic and Lattice Parts of the Order Parameter in a 1D Charge Density Wave System Probed by Femtosecond Spectroscopy, Phys. Rev. Lett. **105**, 066402 (2010).

[43] H. Schaefer, V. V. Kabanov, and J. Demsar, Collective modes in quasi-one-dimensional charge-density wave systems probed by femtosecond time-resolved optical studies, Phys. Rev. B **89**, 045106 (2014).

[44] P. Beaud, A. Caviezel, S. O. Mariager, L. Rettig, G. Ingold, C. Dornes, S.-W. Huang, J. A. Johnson, M. Radovic *et al.*, A time-dependent order parameter for ultrafast photoinduced phase transitions, Nat. Mater. **13**, 923 (2014).

[45] M. Lavagnini, M. Baldini, A. Sacchetti, D. Di Castro, B. Delley, R. Monnier, J.-H. Chu, N. Ru, I. R. Fisher, P. Postorino, and L. Degiorgi, Evidence for coupling between charge density waves and phonons in two-dimensional rare-earth tritellurides, Phys. Rev. B **78**, 201101(R) (2008).